Contributed paper

OPTO-ELECTRONICS REVIEW **12**(1), 111–122 (2004)

Uncooled operation of IR photodetectors

J. PIOTROWSKI*

Military Institute of Armament Technology
7 Prymasa Wyszyńskiego Str., 05-220 Zielonka, Poland

The ultimate performance of long wavelength infrared photodetectors operating at high temperatures is likely to be limited by the noise due to the statistical nature of thermal generation of charge carriers in narrow band gap semiconductors. Additional obstacles to achieve theoretical performance in practical devices arise from weak absorption of infrared radiation, short diffusion length of charge carriers in narrow gap semiconductors and other reasons.

Various ways to improve performance of uncooled photodetector such as the reduction of thermal generation rate by proper selection of the semiconductor material, its doping and suppression of thermal generation by the non-equilibrium mode of operation are considered. Another possibility is the reduction of physical volume of a detector. This can be done by reducing a detector physical area and its thickness with appropriate means to preserve the device field of view and a quantum efficiency.

The advanced architectures of uncooled $Hg_{1-x}Cd_xTe$ IR photoconductors, photoelectromagnetic and photovoltaic detector are described. The devices require heterostructures with complex band gap and doping profiles and can be grown by the low temperature epitaxial techniques. The most promising device for uncooled detection is heterojunction photodiode integrated with optical concentrator. The progress in technology of photodetectors will eventually lead to perfect and fast detection of long wavelength radiation without cooling.

Keywords: infrared photodetectors, uncooled IR photodetectors, MOCVD growth.

1. Introduction

The common believe is that infrared photodetectors of long wavelength radiation need to be cooled to achieve a high sensitivity. The long wavelength IR (LWIR) radiation is characterized by low photon energy. Therefore detection requires electron transitions with threshold energy lower than the photon energy. At near room temperatures the thermal energy of charge carriers becomes comparable to the transition energy resulting in a very high rate of thermal generation of charge carriers. The statistical nature of this process is the source of signal noise. As a result, the long wavelength detectors become very noisy when operated at near room temperature.

Cooling is a direct, straightforward, and the most efficient way to suppress the thermal generation. At the same time cooling is a very impractical method. The need for cooling is a major limitation of photodetectors, and inhibits the more widespread application of infrared technology. Affordable high performance infrared systems require cost-effective infrared detectors that operate without cooling or, at least, operated at temperatures compatible with long-life, low power and low cost coolers.

Since cooling requirements add considerably to the cost, weight, power consumption and inconvenience of an IR system it is highly desirable to eliminate or reduce the cooling requirements. A number of concepts to improve performance of photodetectors operating at near room temperatures have been proposed [1–20]. In principle, the ultimate limits of sensitivity, even for the long wavelength operation, can be achieved without the need for cryogenic cooling.

This paper discusses approaches and technologies aimed at the elimination of cooling requirements of infrared photodetectors operating in the middle 3–8 μm (MWIR) and long 8–14 μm (LWIR) wavelength range of the infrared spectrum.

2. Limitations to performance of infrared photodetectors

2.1. Generalised model

Let us consider a generalized model of a photodetector, in which absorber of infrared radiation with the physical area A_e and the thickness t is coupled by an optical concentrator with its optical area A_o to the beam of infrared radiation [8] (Fig. 1).

The current responsivity of the photodetector is determined by the quantum efficiency, η, and by the photoelectric gain, γ. The quantum efficiency describes how well the

*e-mail: jpiotr@vigo.com.pl

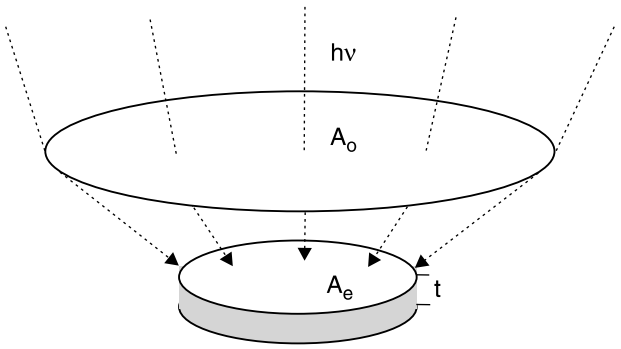

Fig. 1. Model of a photodetector.

detector is coupled to the impinging radiation. It is defined here as the number of electron-hole pairs generated per one incident photon in an intrinsic detector, number of generated free unipolar charge carrier holes in extrinsic detector, or number of charge carriers with energy sufficient to cross potential barrier in the photoemissive detectors. The photoelectric gain is the number of carriers passing contacts per one generated pair in intrinsic detectors (charge carriers in other types of detectors). This value shows how well the generated charge carriers are used to generate current response of a photodetector. Both values are assumed here as constant ones over the device volume.

The spectral current responsivity is

$$R_i = \frac{\lambda\eta}{hc}\gamma q, \tag{1}$$

where λ is the wavelength, h is the Planck constant, c is the velocity of light, q is the electron charge and γ is the photoelectric gain.

In principle, near unity quantum efficiency can be achieved in well-designed infrared photodetectors of any type [8]. Therefore, the signal-to-noise performance is limited by the detector noise. The current that flows through the contacts of the device is noisy due to the statistical nature of generation and recombination processes. Assuming that the current gain for photocurrent and noise current is the same, the noise current is

$$I_n^2 = 2q^2\gamma^2(g+r)\Delta f, \tag{2}$$

where g and r are the total generation and recombination rates in the device, and Δf is the frequency band.

It should be noted that the effects of a fluctuating recombination can frequently be avoided by arranging for the recombination process to take place in a region of the device where it has little effect due to a low photoelectric gain, e.g., at the contacts in sweep-out photoconductors, at backside surface of photoelectromagnetic detector or in the neutral regions of the diodes. The generation processes with their associated fluctuations, however, cannot be avoided by any means [2,3].

Table 1 shows the main sources of the noise presenting limitations to performance of high temperature photodetectors. They can be categorized into three groups: ultimate photon noise limitations, less fundamental limitations due to the thermal generation and technological limitations.

The detectivity, D^*, is the main parameter characterizing normalized signal to noise performance of detectors, and can be defined as

$$D^* = \frac{R_i(A_o\Delta f)^{1/2}}{I_n}, \tag{3}$$

$$D^* = \frac{\lambda\eta}{2^{1/2}hc}\left(\frac{A_o}{g+r}\right)^{1/2}. \tag{4}$$

As we can see, detectivity is dependent on the total generation and recombination rates per unity of the detector

Table 1. Limits to detector performance.

	Noise origin	How to reduce?
Fundamental	Background radiation noise	Spatial and spectral filtering
	Signal photon noise	Cannot be reduced
	Heterodyne photon noise	Cannot be reduced
Less fundamental	Auger thermal generation	Selection of semiconductors, non-equilibrium depletion
	Internal radiative generation	Design of the detector
	Radiative generation from adjacent elements	Design of the detector
Technological	Shockley-Read thermal generation	Improved material technology by elimination of Shockley-Read centres
	Thermal generation at surfaces, interfaces and contacts	Improved processing
	Low frequency noise	Zero bias operation, improved technology
	Amplifier noise	Improved electronic interface

 © 2004 COSiW SEP, Warsaw

optical area. Consider now two important cases of performance limited by external radiation photon noise or by thermal generation/recombination noise.

2.2. Performance limited by external radiation photon noise

The noise of the detector can be determined by a large signal or background radiation photon noise. This frequently happens for the high quality cooled MWIR and LWIR photodetectors that operate at a large thermal background radiation. The generation rate due to the background photon flux Φ_B is

$$g = \eta \Phi_B A_o. \tag{5}$$

Assuming $g = r$

$$I_n^2 = 4q^2\gamma^2 \Phi_B \eta A_o \Delta f, \tag{6}$$

and

$$D^* = \frac{\lambda \eta^{1/2}}{2hc\Phi_B^{1/2}}. \tag{7}$$

As we can see, detectivity of the background limited detector (BLIP) is determined by the photon flux Φ_B and does not depend on a detector optical area.

2.3. Performance limited by thermal generation noise

The BLIP performance is the ultimate goal in development of infrared detectors. The present high temperature photodetectors are typically limited by the thermal generation of charge carriers, however [3–5]. In this case

$$g = GA_e t, \tag{8}$$

$$r = RA_e t, \tag{9}$$

and

$$I_n^2 = 2q^2\gamma^2 (G + R) A_e t \Delta f, \tag{10}$$

where G and R are the volume thermal generation and recombination rates.

The detectivity of the thermal generation-recombination limited device can be expressed as

$$D^* = \frac{\lambda}{2^{1/2} hc} \left(\frac{A_o}{A_e} \right)^{1/2} \frac{\eta}{t^{1/2}} \frac{1}{(G + R)^{1/2}}. \tag{11}$$

As shows Eq. (11), the detectivity can be improved by:
- maximising A_o/A_e,
- maximising $\eta/t^{1/2}$,
- minimising $G + R$.

Let us consider minimizing the $\eta/t^{1/2}$ ratio. It can be shown, that for optimised thickness this ratio is proportional to $\alpha^{1/2}$, where α is to the absorption coefficient. For favourable conditions of double pass of infrared radiation through the detector with negligible/perfect reflection at front/back surfaces of the detector, respectively, the optimised thickness is $0.63/\alpha$. It is worth to note, that the D^* optimised detector is characterized by only ≈76% quantum efficiency, reflecting a tradeoff between requirements of a high quantum efficiency and a low total thermal generation.

D^* of the optimised device is

$$D^* = 0.64 \left(\frac{A_o}{A_e} \right)^{1/2} G_\alpha^{-1/2}, \tag{12}$$

where $G_\alpha = G/\alpha$ is the generation rate within the absorption depth per unity of area. G_α can be considered as the basic figure of merit of any semiconductor material for infrared photodetector of any type.

The ultimate D^*_{BLIP} performance can be achieved with G_α reduced below the level of unavoidable optical generation by the background radiation.

3. Semiconductors for intrinsic photodetectors

3.1. The most important material systems

Table 2 shows the most important material systems used for intrinsic photodetectors such as the binary narrow gap semiconductors, tunable band gap ternary semiconductors, and band gap engineered superlattice materials. The binary compounds can be used for applications that require optimum performance at the spectral range corresponding to band gap of the material. Availability of binary compounds is limited; no one can operate in the LWIR spectral range.

Thermal generation and recombination in narrow gap semiconductors at near room temperature is determined by the Auger mechanism [2–4]. There is no clear indication that some materials among the well known binary alloys and tunable band gap semiconductors are better in terms of the fundamental figure of merit G_α.

$Hg_{1-x}Cd_xTe$ remains to be the champion material among a large variety of material systems [3,4,13]. This is mostly due to extreme flexibility of this material for IR detector applications that makes possible to obtain detector of any type for optimised detection at any region of IR spectrum including, dual and multicolour devices.

Since the Auger generation is dependent on band structure of semiconductor, some new materials may exhibit improved figure of merit due to inherent Auger suppression. An example is InN_xSb_{1-x} with transmission edge wavelengths out to 15 μm at room temperature [16]. It was shown that the Auger recombination rate is about one third that of equivalent band gap $Hg_{1-x}Cd_xTe$, due to the higher electron mass and conduction band non-parabolicity.

Intensive efforts are underway at present on artificial narrow gap semiconductors based on type II and type III

superlattices (see recent review [13] and related papers therein). Reduction of Auger generation rate at room temperature in InAs/GaAs superlattices by nearly one order of magnitude compared to $Hg_{1-x}Cd_xTe$ with similar band gap resulting in detectivity of 1.3×10^8 cmHz$^{1/2}$/W at 11 μm at room temperature has been claimed [15]. No devices of this type are commercially available at present.

Table 2. The most important material systems used for intrinsic photodetectors.

Material system	Most important	Others
Binary alloys	InSb, InAs	PbS, PbSe
Tunable band gap semiconductors	Hg based	$Hg_{1-x}Cd_xTe$, $Hg_{1-x}Zn_xTe$, $Hg_{1-x}Mn_xTe$
	Lead salts	PbSnTe, PbSnSe
	InSb- based	InAsSb, InNSb, InBiTe, InTlSb
Type II superlattices	InAs/GaSb	
Type III supperlattices	HgTe-CdTe	

3.2. $Hg_{1-x}Cd_xTe$

Auger generation rate exponentially increases with increasing temperature and decreasing band gap achieving minimum in lightly p-type doped material [3,4]. Therefore partial suppression of Auger generation can be achieved with careful selection of the band gap and level of doping in dependence on the required spectral response of the photodetector and its operating temperature.

Figures 2 and 3 show numerical optimisation of the active region of $Hg_{1-x}Cd_xTe$ photodetectors. The calculated absorption coefficient in an optimised material decreases with increasing wavelength and is almost independent on temperature. As a result, the optimum thickness increases with in-

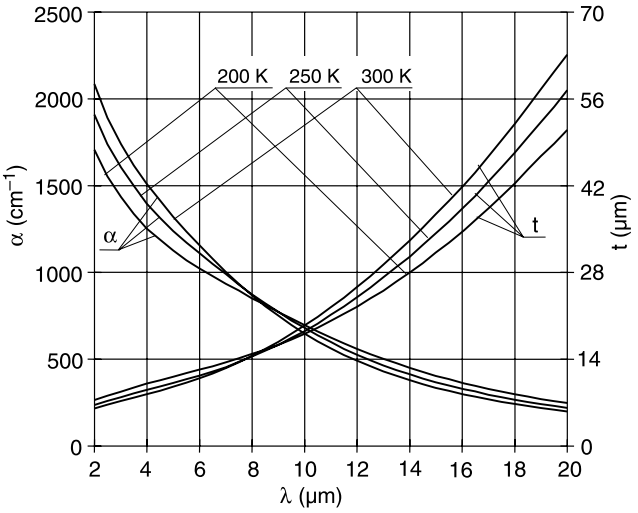

Fig. 2. The calculated absorption coefficient and thickness of optimised photodetectors as a function of operating wavelength and temperature (single pass of radiation).

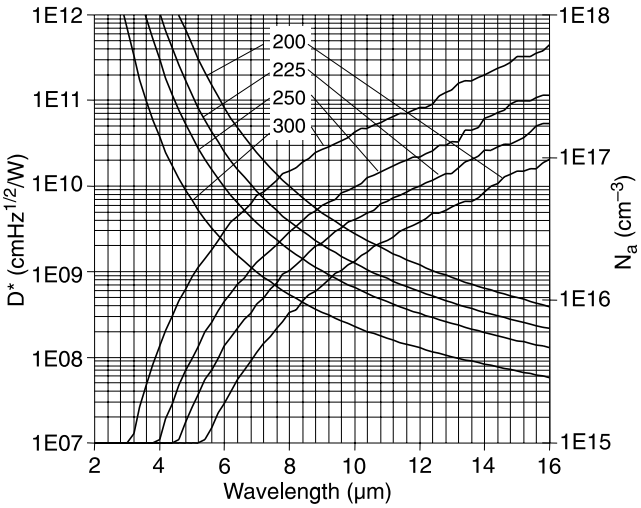

Fig. 3. Ultimate performance of $Hg_{1-x}Cd_xTe$ photodetectors and optimum acceptor doping as a function of wavelength and temperature (double pass of radiation is assumed).

Table 3. Properties of $Hg_{1-x}Cd_xTe$.

Advantages	
Band gap tunability	X, UV, V, SWIR, MWIR and LWIR devices
Lattice constant independent on composition	Easy band gap engineering
Stable n-type doping	Complex doping profiles
Stable p-type doping	Complex doping profiles
Growth on alternative substrates (GaAs, sapphire, silicon) possible	Large area wafers possible, device integrated with optical concentrators and/or with optical resonant cavities
Disadvantages	
Difficult technology	High cost – overcome with progress in epitaxy
Uniformity and reproducibility problems	Arrays non-uniformity
Weak Hg-Te bond	Stability problems – solved with passivation

 © 2004 COSiW SEP, Warsaw

creasing wavelength. Therefore, optimised long wavelength devices operating at near room temperatures would require quite thick active regions. The rule of thumb for selection is the optimum thickness equal to wavelength for double pass of radiation and twice larger for a single pass (both in micrometers). Thickness of ≈20 μm is necessary for optimised single-pass photodetectors operating at λ = 10.6 μm.

Figure 3 shows the calculated detectivity and the optimum doping as a function of wavelength and temperature of operation. The acceptor concentration decreases with decreasing wavelength and temperature. For short wavelength devices operating at the lowest temperature within 200–300 K range, doping less than 1×10^{15} cm^{-3} is required. At the same time, 10^{15} cm^{-3} is the lowest acceptor level achievable in reproducible way at present while low 10^{14} cm^{-3} n-type $Hg_{1-x}Cd_xTe$ can be routinely grown. For this reason, n-type doping is frequently used for some thermoelectrically cooled MWIR devices.

In contrast, the optimum acceptor doping for LWIR devices is well above the 10^{15} cm^{-3} at any temperature within the 200–300 K range. Therefore p-type $Hg_{1-x}Cd_xTe$ is the material of choice for absorbers of LWIR devices.

3.2.1. Non-equilibrium devices

One of the most exciting events in the development of IR photodetectors operating without cryogenic cooling was discovery of Auger suppression [2–4,11,12] decreasing the free carrier concentration below equilibrium values by stationary non-equilibrium depletion of semiconductors. This can be achieved in some devices based on lightly doped narrow gap semiconductors. The examples reverse biased low-high doped (*l-h*) junctions, homo- or heterojunction contact structures, MIS structures or magnetoconcentration effect devices. Under strong depletion the majority carrier concentration saturates at the extrinsic level while the concentration of minority carriers is reduced below the extrinsic level. Therefore the necessary condition for deep depletion is a very light doping of the semiconductor, below the intrinsic concentration.

The non-equilibrium mode of operation may reduce the Auger generation rate by a factor n_i/N_d, where n_i and N_d are the intrinsic and donor concentrations, with improvement of detectivity by $(2n_i/N_d)^{1/2}$. The additional gain factor of $2^{1/2}$ is due to the negligible recombination rate in the depleted semiconductor. The gain for p-type material is even larger, taking into account elimination of Auger 1 and Auger 7 recombination. Additional depletion-related improvement can be also expected from increased absorption due to the reduced band-filing effect.

The resulting improvement may be quite large, particularly for LWIR devices operating at near room temperatures. Potentially, the BLIP performance can be obtained without cooling at all. The BLIP limit for 10-μm device at room temperature can be achieved, by:

- application of materials with controlled doping at a very low levels (≈10^{12} cm^{-3}),
- application of extremely high quality materials with a very low concentration of Shockley-Read centres,
- proper design of the device that prevents thermal generation at surfaces, interfaces and contacts. BLIP performance can be obtained with ≈10^{13} cm^{-3} donor and ≈3×10^{13} cm^{-3} acceptor doping.

The practical devices would require multilayer epitaxial technology capable of growing high-quality heterostructures with complex gap and doping profiles. This technology became available in early nineties and Auger suppressed heterostructural photodiodes have been demonstrated and gradually improved [11].

The present Auger suppressed devices exhibit a high low frequency noise [11,20,21], proportional to the bias current with proportionality coefficient of ≈2×10^{-4}. Since the bias current of the LWIR devices is large, the 1/*f* knee frequencies are 100 MHz to few MHz for ≈10 μm devices at room temperature. This reduces their signal-to-noise ratio at frequencies of 1 kHz to level below that for equilibrium devices! The 1/*f* noise level is much lower in MWIR devices.

The reason for the large 1/*f* noise is not clear. The attempts to find the source of 1/*f* using the perimeter-area analysis give in part contradictory results. The possible routes to reduce the 1/*f* noise is to reduce the dark current or/and the I_n/I ratio with improved material technology and better design of the devices.

4. Practical $Hg_{1-x}Cd_xTe$ photodetectors

4.1. Detector structures

Traditionally, photodetectors are related to one of three groups basing on the principle by which optically generated carriers in the absorber region are sensed [3,4]:

- photoconductors (PC) are electrically biased devices with signal generated in the volume of absorber by the change of its resistance,
- photovoltaic detectors (PV) are unbiased and biased devices with signal generated mostly at homo- or heterojunctions,
- photoelectromagnetic detectors (PEM) are photovoltaic devices based on photoelectromagnetic effect.

Recent advances in heterostructure devices made the distinction between PC and PV devices not so clear, however. Complex heterostructures, frequently with 3D architecture, have been applied for any type of high temperature IR detectors [5]. This is necessary to eliminate unwanted thermal generation and recombination at surfaces, interfaces and contact regions.

A number of specific measures has been applied to improve performance of IR detectors:

- encapsulation of the absorber region with wide gap $Hg_{1-x}Cd_xTe$ to prevent surface and interface generation and recombination,

- heavily n and p-type doped $Hg_{1-x}Cd_xTe$ contact regions to suppress Auger processes and minimize parasitic impedances,
- shielding of the absorber region by metal and dielectric layers to prevent unwanted optical generation by the background thermal radiation,
- backside retroreflectors and, sometimes, optical resonant cavities to reduce the thickness of the absorber without loss of quantum efficiency,
- immersion microoptics to increase the A_o/A_e ratio.

Table 4 shows schematic cross-sections of advanced photodetectors based on $Hg_{1-x}Cd_xTe$ heterostructures epitaxially grown on composite substrates. The devices are typically backside illuminated through the transparent substrate. The drawings reflect main features of the their design. The real structures are usually more complex (3D design, additional layers, optimised grading and other features). Computer simulation is the basic tool to design optimised devices.

4.2. Epitaxial growth

Practical implementation of the advanced photodetector architecture requires well establish epitaxial technology. In Poland, the Isothermal Vapour Phase Epitaxy (ISOVPE) in reusable growth system has been used at VIGO SYSTEM S.A. for a long time to grow $Hg_{1-x}Cd_xTe$ heterostructures on CdZnTe substrates.

Now, the ISOVPE has been replaced with MOCVD (a common investment of VIGO SYSTEM S.A. and Military University of Technology, Warsaw). This technique has been selected for its inherent versatility, low growth temperature, ability to grow layered structures with complex composition and doping profiles while maintaining sharp interfaces. MOCVD (Table 5) makes possible to use low-cost and high quality substrates (GaAs, sapphire and silicon), has the potential for a large-scale production and is cost-effective. Physical properties of MOCVD grown $Hg_{1-x}Cd_xTe$ heterostructures on GaAs exceed those on costly CdTe.

Table 4. Advanced photodetectors based on $Hg_{1-x}Cd_xTe$ heterostructures for near room temperature operation.

Type	Schematic of detector	Features
Photoconductor	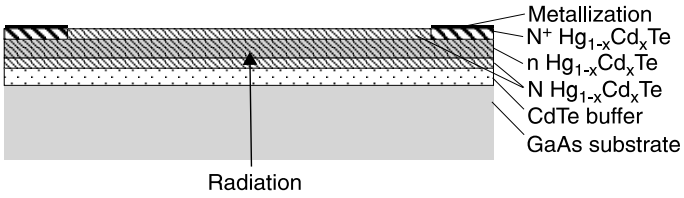	• less costly • high responsivity • bias required
PEM	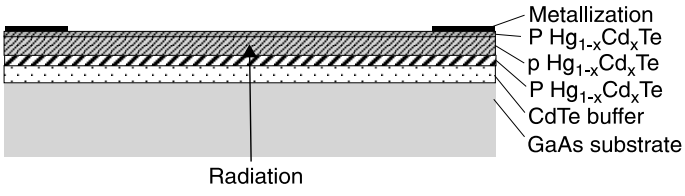	• no bias required • no flicker noise • very short response time • bulky • low performance
Photodiode	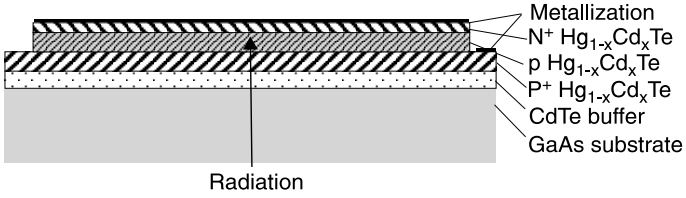	• no bias • fast response • no flicker noise • low resistance • low QE • influence of series resistance
Stacked multi-cell photodiode	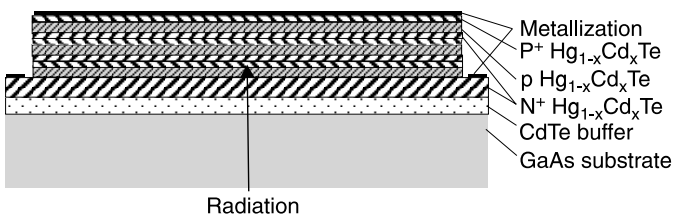	• no flicker noise • DC to very high frequencies • high dynamic resistance • good quantum efficiency • difficult technology

 © 2004 COSiW SEP, Warsaw

Table 5. Comparison of ISOVPE and MOCVD.

Parameter	ISOVPE	MOCVD
Growth temperature	500°C	350–370°C
Substrates: cost availability mechanically thermal conductivity	CdZnTe <$100/cm^2, limited, small wafers soft low	GaAs, sapphire, silicon <$20/cm^2 readily available, large wafers hard high
Uncontrolled doping	$\approx 1\times10^{15}$ cm^{-3}	$<1\times10^{15}$ cm^{-3}
Composition profiles	Graded profiles only	Any, with soft and sharp interfaces
Doping during growth	Possible, but difficult to control	Easy
Complex doping profiles	Difficult	Easy
Throughput	≈ 100 cm^2/month	>1000 cm^2/month

More than 200 growth runs were carried out until now (SEP 2003) and production worthy process for preparation of $Hg_{1-x}Cd_xTe$/CdZnTe/GaAs has been developed. High quality (100) and (111) $Hg_{1-x}Cd_xTe$ heterostructures are grown on 2”(100)GaAs. Reproducible n- and p-type doping at the low, intermediate and high level (10^{15}–10^{18} cm^{-3}) has been achieved with stable iodyne and arsenic dopants. The dopants are easily activated during growth in contrast to MBE. This technology has been used for PC, PEM and PV devices.

4.3. Detector preparation

4.3.1. Detector processing

Since detector processing is largerly integrated with MOCVD growth, the preparation of the detectors include appropriate delineation of active elements, deposition of Au/Cr contacts and passivation. The waferes are then cut with diamond saw into single element devices or small arrays. Some of the devices are supplied with monolithic immersion lenses prepared from GaAs substrates. Individual lenses are prepared with micromachining while photolithography-assisted technology is being used for detector arrays (Fig. 4) [14].

The devices are contacted sapphire fanouts with indium bump-based flip chip technique.

4.3.2. Detector housing

The sensitive elements are housed in various packages, depending on their operating temperature, type of detector, bandwidth and other factors (Fig. 5). Ambient temperature detectors, if properly passivated, can operate in an atmospheric ambient. Sealed housings are necessary for Peltier cooled devices to prevent water vapour condensation, ice deposition and surface contamination. Dry nitrogen, argon and low thermal conductivity krypton-xenon mixtures, are used for 2- and 1-stage thermoelectric coolers. Devices cooled with 3-stage coolers are typically housed in packages filled with dry xenon, which is both an inert and a low thermal conductivity gas. The < 200 K temperature devices require vacuum thermal insulation. TE-cooled devices are supplied with temperature sensors (thermistor or silicon diode) to control the detector temperature.

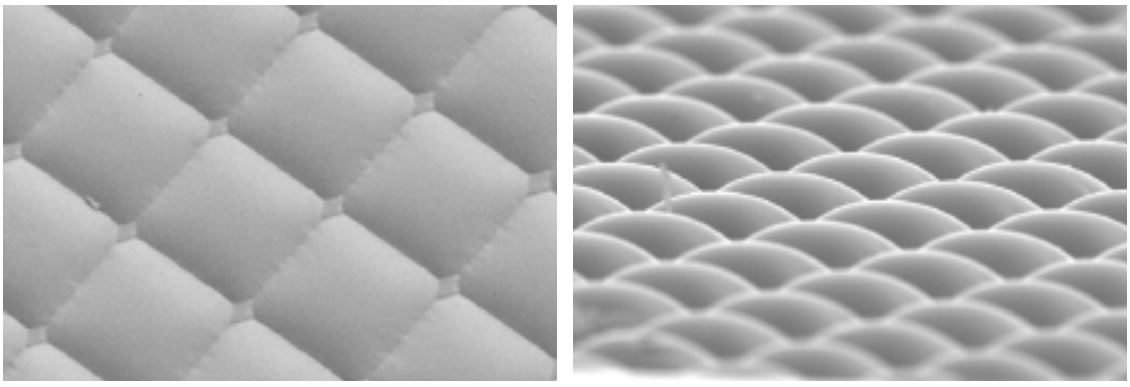

(a) (b)

Fig. 4. SEM images of the microlens array: top (a) and tilted side view (b). The size of the individual lens is 50×50 μm.

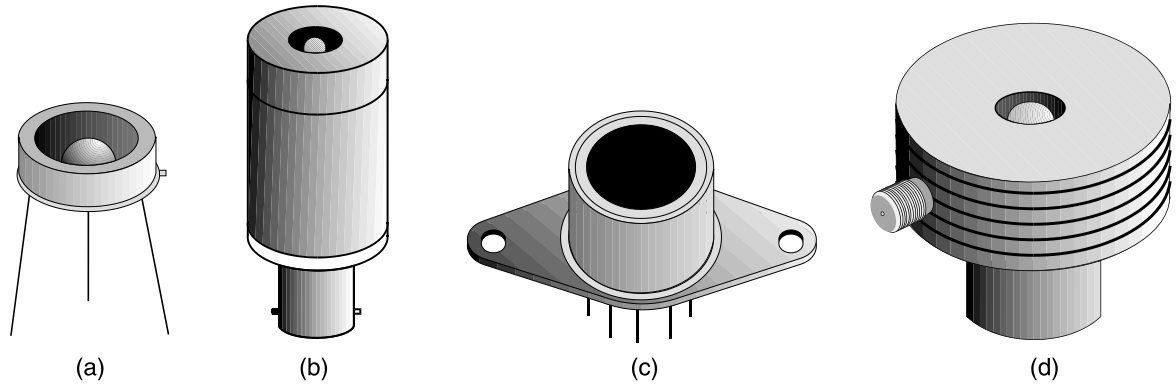

Fig. 5. Housings of optically immersed MWIR and LWIR $Hg_{1-x}Cd_xTe$ photodetectors: uncooled optically immersed photoconductors and photodiodes f <30 MHz (a), uncooled optically immersed photoconductors and photodiodes f >30 MHz (b), Peltier cooled photoconductors, and photovoltaic detectors (c), photoelectromagnetic detectors (d) (after Ref. 22).

4.4. Photoconductive devices

4.4.1. Design

Lightly doped n-type absorber is typically used for thermoelectrically cooled devices operating at wavelength shorter than 5 μm while p-type absorbers are typically used for uncooled > 5 μm and (200–300 K) LWIR devices [1–4]. The absorber region is usually sandwiched between layers with increased band gap that provide heterostructural passivation and supplied with heterojunction contacts. More complex devices with several stacked absorber layers are frequently used to optimise performance in a number of spectral ranges.

4.4.2. Performance

MWIR photodetectors operating at near room temperature at frequencies above the knee frequency fore 1/*f* noise (1–20 kHz) are sub-BLIP devices, limited by G-R noise. The advanced optically immersed MWIR photoconductor detectors operating at temperatures achievable with Peltier coolers closely approach the BLIP limit [23]. This means that the long-term goal of perfect detection of the MWIR radiation at least at temperatures achievable with Peltier cooling has been already achieved.

In practice, detectivities of the LWIR photoconductors still remain below the generation-recombination limit (Table 6) and well below the BLIP limit. The low frequency noise and Johnson-Nyquist thermal noise in uncooled LWIR photoconductors typically exceed the generation-recombination noise so the G-R limit can not be achieved for >10 μm devices. This is especially true for uncooled large area devices. More strong electric fields bias can be applied to small size detectors on substrates with high thermal conductivity where efficient 3D heat dissipation occurs.

In contrast, the G-R limit of performance can be easily achieved in Peltier cooled devices for frequencies above 1/*f* noise knee.

Significant improvement in performance can be obtained by optical immersion. Detectivities exceeding 4×10^9 cmHz$^{1/2}$/W have been obtained in optically immersed devices operating at 10.6 μm wavelength, cooled with two-stage Peltier coolers. Operation of thermoelectrically cooled photoconductive devices has been extended to ≈14 μm, what is important for some Fourier transform spectroscopy and quantum cascade laser based applications.

Uncooled photoconductive devices are not suitable for large area detectors and arrays due to significant heat dissipation. This is especially true for LWIR devices.

4.4.3. Response time

The response time of photoconductors is typically determined by the recombination time in absorber, dependent on the band gap, doping and temperature (Table 7). The high frequency response can be improved employing the sweep out effect, efficient for short length (≈10 μm) devices when transit time is much shorter than the bulk recombination time. Gain-bandwidth product exceeding 1 GHz has been obtained in optically immersed devices with optical area of ≈100×100 μm, operating at 10.6 μm wavelength with two-stage thermoelectric cooling.

Table 6. Above-average detectivities of uncooled and Peltier cooled LWIR (λ = 10.6 μm) photodetectors (in cmHz$^{1/2}$/W).

Detector type	PC		PEM	PV	
Temperature, K	300	225	300	300	225
D* (non-immersed)	6×10^7	2×10^8	2×10^7	6×10^7	4×10^8
D* (immersed)	2×10^8	2×10^9	1.8×10^8	3×10^8	4×10^9

 © 2004 COSiW SEP, Warsaw

Table 7. The response time of $Hg_{1-x}Cd_xTe$ photoconductors.

Spectral range	Cooling	Response time
MWIR (≈5 μm)	Uncooled	≈1 μs
MWIR (≈5 μm)	2 stage Peltier	≈10 μs
LWIR (≈10.6 μm)	Uncooled	≈0.6 ns
LWIR (≈10.6 μm)	2 stage Peltier	≈8 ns

4.5. Photoelectromagnetic (PEM) devices

4.5.1. Design

Typically, the device is three layer heterostructure, with p-type absorber, wider gap P-type layer preventing photogenerated charge carriers to recombine and a thin, narrow gap p-type layer to increase recombination of charge carriers at the interface between absorber and this layer. The active elements are placed in strong magnetic field (≈2 T) that is achievable with miniature permanent magnets.

4.5.2. Performance

PEM detectors device are usually used for detection of LWIR radiation at room temperature since bulky magnet (≈1 cm^3) makes Peltier cooling difficult [1,4,7]. The main limitation of PEM detectors is poor quantum efficiency due to a weak absorption of long wavelength radiation. Only small fraction of incoming radiation can be absorbed within the diffusion length where photogenerated charge carriers contribute to the electrical signal.

4.5.3. Response time

PEM detectors have excellent frequency response. Since typical thickness of the absorber region is close to the diffusion length or shorter, the effective recombination time is limited by the diffusion of photogenerated carriers to the surface of a high recombination velocity. Due to a high ambipolar mobility in narrow gap p-type $Hg_{1-x}Cd_xTe$ and a small thickness of the absorber region, the diffusion time can be very short. The RC time is also very short due to a low sheet resistance (≈50 ohms) and small capacitance (<1 pF). With proper optimisation, the response time can be shorter than < 100 ps.

Although PEM devices have relatively modest performance, they are very useful for many applications due to inherent important advantages: no electric bias, no low frequency noise, relatively large maximum output voltages, and very good frequency response.

4.6. Photovoltaic devices

4.6.1. Design

The n^+-p homojunction or n^+-p-P heterojunction structures were used in the past for near room temperature photovoltaic detectors while the present PV devices are usually based on the three-layer N^+-p-P^+ or more complex heterostructures [3,5,23]. Light p-type doping is used for absorber region. Heavily doped N^+ layer provides the base contact with a very low resistance (few ohms). The top contact is a heavily doped P^+-type layer. This layers is covered with contact metallisation that also plays a role of retroreflector inducing double pass of infrared radiation. Additional layer are also used to reduce G-R and tunnel currents generated at interfaces [20,23].

The thickness of the buffer and other layers within the device is frequently selected to achieve the optical resonance in a required spectral range. Optical immersion is typically used to improve performance, increase resistance and reduce capacitance. Figure 6 shows schematic cross section of mesa photodiodes monolithically integrated with immersion lenses.

The single-cell devices can be successfully used only for small area uncooled and Peltier cooled devices operating in the MWIR spectral range. The long wavelength photovoltaic devices operating at near room temperature suffer from poor quantum efficiency and low differential resistance [6,8–10].

Only the charge carriers that are photogenerated at distance shorter than the diffusion length from junction can be collected. Since the absorption depth of long wavelength IR radiation ($\lambda > 5$ μm) is longer than the diffusion length, only a limited fraction of the photogenerated charge can contribute to the quantum efficiency.

Consider an example of an uncooled 10.6 μm photodiode. Calculations show that the ambipolar diffusion length is less than 2 μm while the absorption depth is ≈13 μm. This reduces the quantum efficiency to ≈15% for a single pass of radiation through the detector.

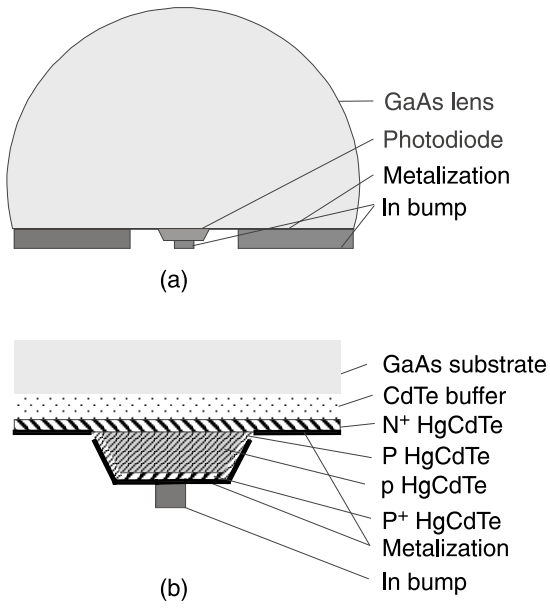

Fig. 6. Schematic cross-section of optically immersed 10.6 μm mesa photodiode for operation at 200–300 K: complete structure (a) and enlarged view of active element (b).

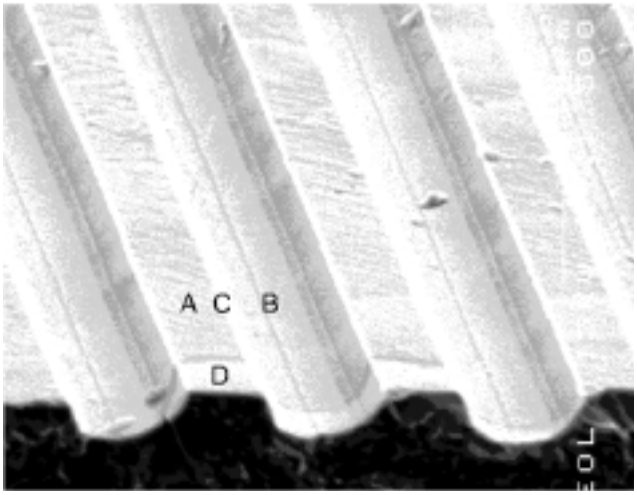

Fig. 7. SEM images of a multi-heterojunction photodetector: plan view of the whole device. A – mesa structure, B – trenches, C – non-metallised wall, D – non-metallised region of the device.

The resistance of the p-n junction is very low due to a high thermal generation and ambipolar effects [2–4]. As a result, the noise of parasitic device resistances and preamplifier noise may exceed the thermal generation-recombination noise.

The two problems make the single-cell uncooled LWIR devices not usable for practical applications. These problems have been solved through adoption of sophisticated architecture of photovoltaic detectors [8–10,14,17,19] based on multiple heterojunctions. One solution is device with junctions perpendicular to the surface (Fig. 7) used in practice by VIGO SYSTEM S.A. since 1995. They are the only uncooled and unbiased long wavelength photovoltaic devices commercially available at present. Such devices suffer from the non-uniform response across the active area, occurrence of dead regions and dependence of response on polarization of incident radiation.

More promising are the stacked multijunction photodiodes shown in Fig. 8 [19]. The devices are multiple three- layer (or more) heterojunction cells, monolithically connected in series.

The general rules to optimise performance of the device are:

- absorber materials should be optimised for the maximum ratio of the absorption coefficient to the thermal generation rate,
- the thickness of the absorber region of each cell should be less than the ambipolar diffusion length to ensure a good collection of photogenerated carriers,
- the combined thickness of all absorber regions must be comparable to the absorption depth of infrared radiation of the wavelength for which the device is optimised. This ensures near 100% use of incident photons.

Such devices are capable to achieve good quantum efficiency, large differential resistance, and fast response. The potential problem in practical implementation is a low resistance connection of N^+ and P^+ regions of adjacent cells in the device. This can be achieved employing band gap engineered design employing tunneling between at the N^+ and P^+ interface.

4.6.2. Performance

Photovoltaic detectors are characterized by inherent advantages in comparison to photoconductors and photoelectromagnetic detectors. They do not require electric nor magnetic bias, show no low frequency bias and can operate from DC to very high frequencies.

The performance of the photovoltaic detectors based on optimised $Hg_{1-x}Cd_xTe$ heterostructures is similar to that of photoconductors operating at the same conditions (Fig. 9).

Without optical immersion MWIR photovoltaic detectors are sub-BLIP devices with performance close to the *G-R* limit. Only well designed optically immersed devices approach BLIP limit when thermoelectrically cooled with 2-stage Peltier coolers.

Situation is even less favourable for LWIR photovoltaic detectors. Despite of all improvements (advanced architecture, optical immersion, Peltier cooling) they show detectivities below the BLIP limit by almost one order of magnitude. The detectivities exceeding 1×10^9 cmHz$^{1/2}$/W and 6×10^9 cmHz$^{1/2}$/W have been measured with uncooled

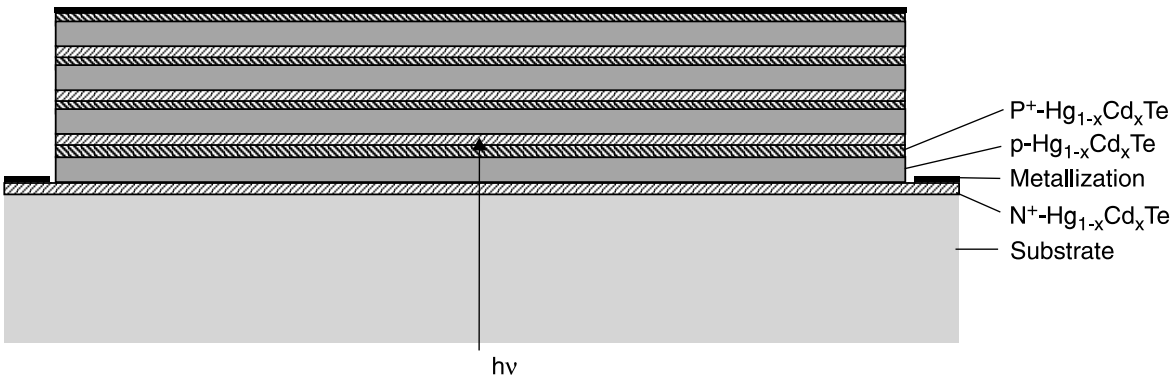

Fig. 8. Schematic cross-sections of single N^+-p-P^+ heterojunction photodiode cell (a) and the 4-cells stacked multiple detector (b). The backside illuminated device is supplied with reflector for double pass of IR radiation.

 © 2004 COSiW SEP, Warsaw

λ = 8.5 μm non-immersed and optically immersed devices, respectively [14,17,22,23]. Optically immersed 10.6 μm P^+-p-N^+ device cooled with 2-stage Peltier cooler with detectivities of ≈ 4×10^9 cmHz$^{1/2}$/W has been also reported [17].

In contrast to photoconductors, photodiodes, with their very low power dissipation, can be assembled in two-dimensional arrays containing a very large (≈10^6) number of elements, limited only by existing technologies.

4.6.3. Response time

The frequency response of photovoltaic devices is limited by transport of photogenerated charge carriers through the absorber region and by RC time constant.

Transport through the absorber region is a combination of diffusion and drift. The p-type $Hg_{1-x}Cd_xTe$ is the material of choice for an absorber of a fast photodiode due to a large diffusion coefficient of electrons. The diffusion transit times at room temperature are ≈100 ps for extrinsic p-type 3-μm thick $Hg_{0.835}Cd_{0.165}Te$ absorber. Further reduction can be achieved with thinner absorber. Drift transport in reverse biased devices can reduce the transit time further.

The main limitation of response time is usually the RC time constant. For transimpedance preamplifier with a low input resistance, the RC time constant is determined by the junction capacitance and the photodiode series resistance. Reduction of series resistance by almost two orders of magnitude is possible using structures with heavily doped n-type material for the mesa base layer, with corresponding reduction of the RC time constant.

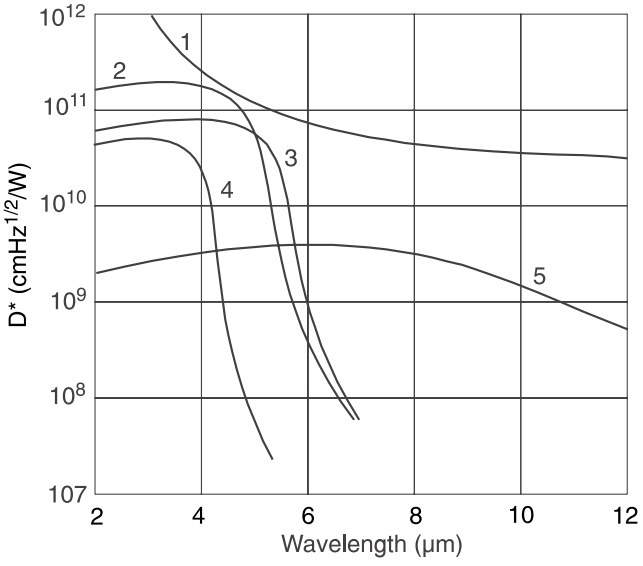

Fig. 9. Spectral detectivity of advanced photoconductors and photovoltaic devices: 1 – background limit D_{BLIP}*(300 K, 180°), 2 – PCI-2TE-5, 3 – PDI-2TE-5, 4 – PDI-4, 5 – PCI-2TE-10.6 (After Ref. 23). The symbols stand for: PC – photoconductive, PV – photovoltaic, I – optically immersed, 2TE – two-stage Peltier cooling.

A very short RC time constant is expected in optically immersed photodiodes with very small area of active region. With these improvements photodiodes can be use for gigahertz range detection of IR radiation.

5. Conclusions

As theoretical analysis show, there is no fundamental obstacle to perfect detection of MWIR and LWIR radiation without cryogenic cooling. The problems are of technological rather than fundamental nature. The practical uncooled devices still present a challenge, but they have been steadily improved.

Where we are now?

- thermoelectrically cooled and optically immersed MWIR photodetectors closely approach the BLIP limit,
- the best optically immersed equilibrium mode LWIR devices cooled with two-stage Peltier coolers are by one order of magnitude below the BLIP limit of performance,
- the best non-immersed Auger suppressed LWIR devices are also by one order of magnitude below the background limit of performance at frequencies above 1/*f* knee. Although the non-equilibrium mode Auger suppression seems to be a viable approach to drive the operating temperature of the photodetectors into the uncooled regime, reduction of the background acceptor doping below 10^{14} cm^3 and trap concentration below ≈10^{13} cm^{-3} is required for BLIP performance at λ = 10 μm. The requirement for doping are softened by almost one order of magnitude for 4 μm devices. In contrast, trap concentration requirements are even more stringent for MWIR devices,
- the performance of the Auger suppressed devices can be improved further by the use of optical immersion and the resonant optical cavity. Apart from the usual gain in performance, optical immersion highly reduces the total bias power dissipation, which would be important in large size elements and in future multi-element arrays of extracted photodiodes. Another advantage is significant reduction of radiative exchange between adjacent element in an array. The arrangement of the photodiode in the optical resonant cavity makes it possible to use a thin extracted zone without loss in quantum efficiency, which is also favourable for reduction of saturation current and results in minimising noise and bias power dissipation,
- the combination of the improvements should lead to BLIP performance already with technologies available at present.

The near room temperature photodetectors have found increasingly widespread civilian (pyrometry and thermography, gas analysis with conventional, laser and Fourier transform spectroscopy, free space high transfer rate optical communications; test equipment) and military (night vision, laser range finder and threat warning devices, gun sights, smart munitions) applications.

The elimination of cooling will lead to significant reduction in cost, logistical supply, and an increase in the mean time between failures.

Acknowledgements

The work was performed, in part, under the Polish Committee for Scientific Investigation Grant No. KBN-0T00A00521.

References

1. J. Piotrowski, W. Galus, and M. Grudzien, "Near room-temperature IR photodetectors", *Infrared. Phys.* **31**, 1–48 (1990).
2. T. Elliott, "Non-equilibrium modes of operation of narrow-gap semiconductor devices", *Semicond. Sci. Technol.* **5**, S30–S37 (1990).
3. C.T. Elliott and N.T. Gordon, "Infrared Detectors", in *Handbook on Semiconductors*, Vol. 4, pp. 841–936, edited by C. Hilsum, North-Holland, Amsterdam, 1993.
4. J. Piotrowski. "$Hg_{1-x}Cd_xTe$ infrared photodetectors", in *Infrared Photon Detectors*, 391–494, edited by A.. Rogalski, SPIE Press, Bellingham, 1995.
5. J. Piotrowski and M. Razeghi, "Improved performance of IR photodetectors with 3D gap engineering", *Proc. SPIE* **2397**, 180–192 (1995).
6. K. Adamiec, M. Grudzien, Z. Nowak, J. Pawluczyk, J. Piotrowski, J. Antoszewski, J. Dell, C. Musc, and L. Faraone, "Isothermal vapour phase epitaxy as a versatile technology for infrared photodetectors", *Proc. SPIE* **2999**, 34–43 (1997).
7. J. Piotrowski and A. Rogalski: "Photoelectromagnetic, magnetoconcentration and Dember infrared detectors", in *Narrow Gap II-VI Compounds for Optoelectronic and Electromagnetic Applications*, edited by P. Capper, Chapman and Hall, London, 1997.
8. J. Piotrowski and W. Gawron, "Ultimate performance of infrared photodetectors and figure of merit of detector material", *Infrared Phys. Technol.* **38**, 63–68 (1997).
9. C. Musca, J. Antoszewski, J. Dell, L. Faraone J. Piotrowski, and Z. Nowak, "Multi-junction HgCdTe long wavelength infrared photovoltaic detector for operation at near room temperature", *J. Electr. Mat.* **27**, 740–746 (1998).
10. J. Piotrowski, Z. Nowak, J. Antoszewski, C. Musca, J. Dell, and L. Faraone, "A novel multi-heterojunction HgCdTe long-wavelength infrared photovoltaic detector for operation under reduced cooling conditions", *Semicond. Sci. Technol.* **13**, 1209–1214 (1998).
11. T. Elliott, N.T. Gordon, and A..M. White "Towards background-limited, room-temperature, infrared photon detectors in the 3–13 μm wavelength range", *Appl. Phys. Lett.* **74**, 2881–2883 (1999).
12. M.A. Kinch, "Fundamental physics of infrared detector materials", *J. Electron. Mater.* **29** 809-817 (2000).
13. A. Rogalski, K. Adamiec, and J. Rutkowski, *Narrow Gap Semiconductor Photodiodes*, SPIE Press, Bellingham, 2000.
14. J. Piotrowski, M. Grudzień, Z. Nowak, Z. Orman, J. Pawluczyk, M. Romanis, and W. Gawron, "Uncooled photovoltaic $Hg_{1-x}Cd_xTe$ LWIR detectors", *Proc. SPIE* **4130**, 175–184 (2000).
15. H. Mohseni, J. Wojkowski, M. Razeghi, G. Brown, and W. Mitchel, "Uncoded InAs–GaSb type–II infrared detectors grown on GaAs substrates for the 8–12 μm atmospheric window", *IEEE J. Quant. Electron.* **35**, 1041–1044 (1999).
16. N. Murdin, M. Kamal-Saadi, A. Lindsay, E.P. O'Reilly, and A.R. Adams, G.J. Nott, J.G. Crowder, and C.R. Pidgeon, I.V. Bradley, and J.-P.R. Wells, T. Burke, A.D. Johnson, and T. Ashley. "Auger recombination in long-wavelength infrared InN_xSb_{1-x}", *Appl. Phys. Lett.* **78**, 1568–1570 (2001).
17. J. Piotrowski, "Suppression of Auger generation as the way to perfect detection of infrared radiation", *Armament Technology Problems* **82**, 57–68 (2002). (in Polish).
18. J. Piotrowski, "Uncooled IR photodetectors get a performance boost", *Photonics* **37**, 97–99 (2003).
19. J. Piotrowski, P. Brzozowski, and K. Jóźwikowski, "Stacked multijunction photodetectors of long wavelength radiation", *J. Electron. Mat.* **32**, 672–676 (2003).
20. M.K. Ashby, N. T. Gordon, C. T. Elliott, C.L. Jones, C.D. Maxey, L. Hipwood, and R. Catchpole, "Investigation into the source of 1/*f* noise in $Hg_{1-x}Cd_xTe$ diodes", *U.S. Workshop on the Physics and Chemistry of II–VI Materials, Extended Abstract*, 127–130 (2003).
21. C.L. Jones, N.E. Metcalfe, A. Best, R. Catchpole, C.D. Maxey, N.T Gordon, R.S. Hall, T. Colin, and T. Skauli, "Effect of device processing on 1/*f* noise in uncooled, Auger-ssuppressed CdHgTe diodes", *J. Electr. Mat.* **27**, 733–739 (1998).
22. Vigo Systems Data Sheets 2000, www.vigo.com.pl.
23. Vigo Systems S.A. Unpublished results (2003).

 © 2004 COSiW SEP, Warsaw